

Hidden quantum mirage by negative refraction in semiconductor P-N junctions

Shu-Hui Zhang¹, Jia-Ji Zhu³, Wen Yang^{1,*}, Hai-Qing Lin¹, and Kai Chang^{2,4†}

¹*Beijing Computational Science Research Center, Beijing 100094, China*

²*SKLSM, Institute of Semiconductors, Chinese Academy of Sciences, P.O. Box 912, Beijing 100083, China*

³*Institute for quantum information and spintronics, College of Science, Chongqing University of Posts and Telecommunications, Chongqing 400065, China and*

⁴*Synergetic Innovation Center of Quantum Information and Quantum Physics, University of Science and Technology of China, Hefei, Anhui 230026, China*

We predict a novel quantum interference based on the negative refraction across a semiconductor P-N junction: with a local pump on one side of the junction, the response of a local probe on the other side behaves as if the disturbance emanates not from the pump but instead from its mirror image about the junction. This phenomenon is guaranteed by translational invariance of the system and matching of Fermi surfaces of the constituent materials, thus it is robust against other details of the junction (e.g., junction width, potential profile, and even disorder). The recently fabricated P-N junctions in 2D semiconductors provide ideal platforms to explore this phenomenon and its applications to dramatically enhance charge and spin transport as well as carrier-mediated long-range correlation.

PACS numbers: 73.40.Lq, 75.30.Hx, 72.80.Vp

Half a century ago, Veselago proposed the concept of negative refraction for electromagnetic waves [1–4]: upon transition from a medium with positive refractive index across a sharp interface into a negative index medium, a diverging pencil of rays is coherently refocused to form a sharp image or “quantum mirage” [5], similar to the bending of light to create mirages in the atmosphere. In the past decade, negative refraction and mirage have been observed for electromagnetic waves of various frequencies (see Ref. [6] for a review) and for cold atoms [7, 8]. In 2007, Cheianov *et al.* [9] proposed the interesting idea that a sharp P-N junction of graphene can exhibit negative refraction and hence focus electrons out of a local pump into a sharp quantum mirage. This effect has been widely used in theoretical proposals to control charge and/or spin transport for massless Dirac fermions in semiconductors (see Refs. [10–12] for a few examples). However, a sharp quantum mirage requires the junction to be sharp compared with the electron wavelength (\sim a few nanometers), otherwise it would disappear due to the path-dependent phase accumulation inside the junction. This makes the observation and application of this effect an experimentally challenging task [13].

In this letter, we theoretically demonstrate that in many situations where the quantum mirage is no longer visible, its effect still exists, which could make the response across the P-N junction independent of distance. As a basic observation in physics, the response amplitude in a d -dimensional uniform system decays at least as fast as $1/R^{(d-1)/2}$ with distance R , irrespective of the energy dispersion, spin-orbit coupling, etc. This directly leads to rapid decay of many physical properties, such as the charge and spin conductivity [14] (response to

electric/magnetic field), nonlocal optical response [15], Friedel oscillation [16–18] (response to charge impurity), and carrier-mediated Rudermann-Kittel-Kasuya-Yosida interaction [19–22] (response to magnetic impurity). The *hidden* quantum mirage could lift these constraints and dramatically enhance the nonlocal responses for electrons in various semiconductors such as graphene, silicene, transition-metal dichalcogenides, topological insulator surfaces, etc. As an example, we demonstrate that the P-N junction could dramatically enhance the carrier-mediated long-range interaction between localized magnetic moments by several orders of magnitudes.

For an intuitive physical picture about the hidden quantum mirage, we start from a sharp P-N junction as shown in Fig. 1(a). Here the plane waves excited by a local pump (filled red circle) in the N region is perfectly focused by the junction into a sharp quantum mirage (red dashed circle) in the P region [9, 13]. Consequently, when a local probe (filled blue circle) is scanned in the P region, the probe only “sees” the mirage. This motivates the natural expectation that the response of the probe would behave as if the disturbance originated from this mirage instead of the pump. When the interface becomes sufficiently smooth or disordered [see Fig. 1(b)], however, the quantum mirage disappears. Surprisingly, the pump-probe response is still independent of their distances when the pump and probe undergo equal shifts in opposite directions perpendicular to the interface, *as if the quantum mirage were still there*.

To understand this *robust, hidden* quantum mirage effect, from now on we specialize to P-N junctions (PNJs) of two-dimensional semiconductors. The PNJ under consideration has translational invariance along its interface [y axis, see Fig. 1(b)] and one electron (hole) Fermi surface in the N (P) region [Figs. 1(c) and (d)]. Apart from this, the PNJ is arbitrary, e.g., the junction could be homo or hetero, sharp or smooth, with arbitrary and

* wenyang@csrc.ac.cn

† kchang@semi.ac.cn

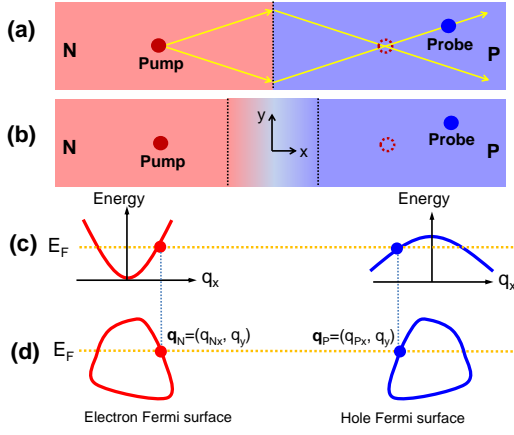


FIG. 1. (color online). (a) In a sharp P-N junction, a local pump (filled red circle) in the N region generates a sharp quantum mirage (dashed red circle) in the P region through negative refraction. The response of a local probe (filled blue circle) in the P region behaves as if the disturbance emanates not from the pump but instead from the quantum mirage. (b) In a smooth P-N junction, the sharp quantum mirage disappears, but its effect still exists. (c) Sketch of the electron energy band in the N region and hole energy band in the P region. (d) Fermi surface matching: the mirror reflection of the electron Fermi surface (red curve) about the junction interface coincides with the hole Fermi surface (blue curve).

even random potential profile. A right-going plane wave $e^{i\mathbf{q}_N \cdot \mathbf{r}}$ with momentum $\mathbf{q}_N \equiv (q_{N,x}, q_y)$ ($q_{N,x} > 0$) [red spot in Fig. 1(c) and (d)] on the electron Fermi surface goes across the junction and becomes a right-going transmitted wave $e^{i\mathbf{q}_P \cdot \mathbf{r}}$ with momentum $\mathbf{q}_P \equiv (q_{P,x}, q_y)$ ($q_{P,x} < 0$) [blue spot in Fig. 1(c) and (d)] on the hole Fermi surface. The response amplitude (as quantified by the retarded propagator on the Fermi surface) of the probe located at \mathbf{R}_2 [filled blue circle in Fig. 1(b)] in the P region due to a local pump located at \mathbf{R}_1 [filled red circle in Fig. 1(b)] in the N region is dominated by these plane waves on the Fermi surface (see supplementary online materials):

$$G(\mathbf{R}_2, \mathbf{R}_1) = \int \frac{dq_y}{2\pi} w(q_y) e^{i(\mathbf{q}_P \cdot \mathbf{R}_2 - \mathbf{q}_N \cdot \mathbf{R}_1)}, \quad (1)$$

where $w(q_y)$ is the transmission amplitude across the junction and $e^{i(\mathbf{q}_P \cdot \mathbf{R}_2 - \mathbf{q}_N \cdot \mathbf{R}_1)}$ is the phase factor associated with the propagation outside the junction. Note that the details of the junction (breadth, potential profile, etc) only influences $w(q_y)$ and has no effect on the propagation phase factor outside the junction. For uniform systems, we have $\mathbf{q}_N = \mathbf{q}_P \equiv \mathbf{q}$, so the response only depends on the displacement $\mathbf{R}_2 - \mathbf{R}_1$ between the pump and the probe: the rapid oscillation of the propagation phase factor $e^{i\mathbf{q} \cdot (\mathbf{R}_2 - \mathbf{R}_1)}$ at large distances leads to destructive interference and hence $1/R^{1/2}$ decay of the response with the pump-probe distance $R \equiv |\mathbf{R}_2 - \mathbf{R}_1|$, which is just the $d = 2$ case of the usual $1/R^{(d-1)/2}$ decay

in a uniform d -dimensional conducting system.

For PNJs, an interesting phenomenon appears when the mirror reflection of the electron Fermi surface about the junction coincides with the hole Fermi surface [Fig. 1(d)], so that

$$q_{N,x} = -q_{P,x}$$

for all q_y . For such Fermi-surface-matched PNJs, the propagation phase factor becomes $e^{iq_y(Y_2 - Y_1)} e^{-iq_{N,x}(X_2 + X_1)}$, so the response depends on the pump location $\mathbf{R}_1 \equiv (X_1, Y_1)$ and probe location $\mathbf{R}_2 \equiv (X_2, Y_2)$ through $Y_2 - Y_1$ and $X_2 + X_1$ only. In other words, the response of the probe remains invariant not only upon identical displacement of the pump and probe parallel to the junction (this invariance trivially follows from the translational symmetry of the system along the junction), but also upon opposite displacement of the pump and the probe perpendicular to the junction (this invariance is absent from the Hamiltonian and originates from Fermi surface matching), as if the disturbance emanated *not* from the pump but instead from its *mirror point* about the junction [dashed red circle in Fig. 1(b)] although the conventional quantum mirage [6–9, 13] already disappears.

The key to this hidden quantum mirage effect is that the momenta of the propagating electrons (on the Fermi surface) in the N region and P region are identical along the junction, but opposite perpendicular to the junction. As a result, when the pump and probe are moved in opposite directions perpendicular to the junction by an equal amount ΔX , the extra propagation phase factor $e^{iq_{P,x}\Delta X}$ in the P region is exactly cancelled by the extra propagation phase factor $e^{iq_{N,x}\Delta X}$ in the N region. Even when Fermi-surface matching is slightly broken, this physical picture could still guarantee weak dependence of the non-local response on the pump-probe distance.

This hidden quantum mirage effect has two distinguishing features compared with various conventional quantum mirages, such as electrostatic lens [23], refocusing by an elliptical quantum corral [5], and refocusing by negative refraction [8, 9, 13]. First, it follows entirely from symmetries (Fermi surface matching and 1D translational invariance). Second, it cannot be directly observed as a mirage (i.e., local enhancement of the probe response), but instead manifests itself as a distance-independent response. This effect is applicable to either massless or massive electrons in a wide range of materials. It also applies to other matter waves and electromagnetic waves, thus the many experimental platforms [8, 13, 24–29] that have been used for observing the refocusing by negative refraction for various matter waves could be used to observe this more robust phenomenon.

Since the most popular 2D semiconductors have isotropic low-energy dispersion, Fermi surface matching can be satisfied by appropriately tuning the Fermi energy, so that the hidden quantum mirage can be detected by the well-developed multiprobe scanning tunneling microscopy (STM), which has already been used

to characterize the non-local responses of many systems [30] such as two-dimensional thin films [31] and graphene [32, 33] with nanoscale resolution. We consider a two-dimensional PNJ connected to two STM tips, one located at \mathbf{R}_1 in the N region and the other at \mathbf{R}_2 in the P region. The zero-temperature conductance is given by the Landauer formula [34] as $G_C = (2e^2/h)T$, where

$$T = |G(\mathbf{R}_2, \mathbf{R}_1)|^2 \Gamma_1 \Gamma_2$$

is the transmission coefficient and Γ_i ($i = 1, 2$) is the coupling to the i th probe. For uniform systems, the conductance decays as $1/R$ with distance $R \equiv |\mathbf{R}_2 - \mathbf{R}_1|$ due to the universal decay $G(\mathbf{R}_2, \mathbf{R}_1) \propto 1/R^{1/2}$. In a Fermi-surface matched PNJ, the conductance would be distance-independent when the two STM tips are moved oppositely perpendicular to the junction. When the material has significant spin splitting, e.g., due to intrinsic spin-orbit coupling or by external exchange field from a ferromagnetic layer [11], the Fermi surface matching may occur for only one spin orientation, then the hidden quantum mirage becomes spin-selective. This can be detected by spin-polarized STM [35, 36].

In addition to charge and spin transport, the hidden quantum mirage is also applicable to carrier-mediated Rudermann-Kittel-Kasuya-Yosida (RKKY) interaction between distant localized spins. In d -dimensional systems, the RKKY interaction decays rapidly as $1/R^d$ with the inter-spin distance R [37], limiting the spatial range of spin-spin correlation on 2D systems that can be directly detected via spin-polarized scanning tunneling microscopy to a few nanometers [36, 38]. This universal decay of the RKKY interaction strength $J \sim G^2(\mathbf{R}_2, \mathbf{R}_1)/R$ is a direct consequence of the $1/R^{(d-1)/2}$ decay of the nonlocal response. Thus the hidden quantum mirage could slow down the decay of the RKKY interaction from $1/R^d$ to $1/R$, and hence drastically enhances its magnitude.

With the rapid progress in modern nanotechnology, high-quality PNJs have been fabricated in graphene [13, 39–41], transition-metal dichalcogenides [42–44], and are under development for topological insulator surfaces [45, 46]. We have performed extensive numerical simulation that demonstrate the existence of hidden quantum mirage in these systems (graphene, monolayer MoS₂, and topological insulator surfaces). Here we present our results for graphene based on the tight-binding model. For brevity, we use the lattice constant $a = 1.42$ Å (nearest-neighbor hopping constant $t \approx 3$ eV) of graphene as the unit of length (energy).

As illustrated in Fig. 2, voltages applied to the top and back gates shift the electron Dirac cones down by V_0 on the left (N region) and up by V_0 on the right (P region), so that Fermi surface matching is achieved. As shown in Fig. 3(a) and (b), when we move the pump and probe, initially at $\mathbf{R}_1 = \mathbf{R}_2 = (-60, 0)$ in the N region, in opposite directions along the x axis with $X_2 + X_1$ fixed, the pump-probe response amplitude initially oscillates and decays, but becomes invariant after the probe

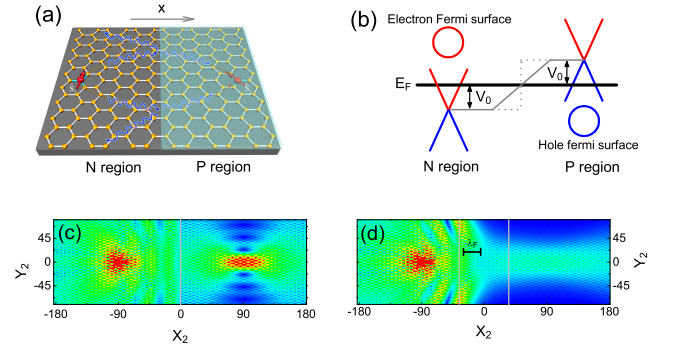


FIG. 2. (color online). (a) Graphene PNJ along the zigzag direction. (b) The gate voltages shift the Dirac cone of the N (P) region by $-V_0$ ($+V_0$). The N and P regions are spatially separated by a sharp (green dashed line) or smooth linear (green solid line) junction, whose interfaces are indicated by the vertical gray lines. Fermi surface matching occurs when the Fermi level locates midway in between the Dirac points, i.e., $E_F = 0$. (c) shows the well-known quantum mirage for a sharp junction: with a pump at $\mathbf{R}_1 = (-91, 0)$, the response of a scanning probe $\mathbf{R}_2 = (X_2, Y_2)$ shows a sharp maximum at the mirror point $(+91, 0)$. (d) shows that the quantum mirage gradually disappears when the junction is wider than the Fermi wavelength λ_F . In all the calculations $V_0 = 0.2$.

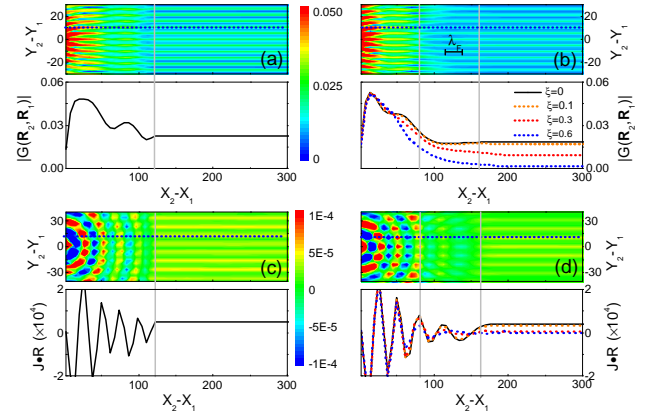


FIG. 3. (color online). (a) and (b): contour plot of pump-probe response amplitude $|G(\mathbf{R}_2, \mathbf{R}_1)|$ vs. $\mathbf{R}_2 - \mathbf{R}_1$ for fixed $X_2 + X_1 = -120$ in (a) sharp or (b) smooth PNJ. A horizontal slice (blue dashed line) of the contour plot is shown as the black solid lines in the lower panel. The dashed lines in the lower panel of (b) include on-site disorder of different strengths $\xi = 0.1, 0.3$, and 0.6 along the x axis in the junction region. (c) and (d): similar to (a) and (b), but for the scaled RKKY interaction JR . In all the calculations $V_0 = 0.2$.

enters deep into the P region. Such distance-independent response occurs not only in a sharp PNJ [Fig. 3(a)], but also in a smooth PNJ with junction width \gg carrier Fermi wavelength λ_F [Fig. 3(b)], even when on-site disorder of various strengths $\xi = 0.1, 0.3$, and 0.6 along the x axis in the junction region has been introduced [dashed lines in the lower panel of Fig. 3(b)]. This

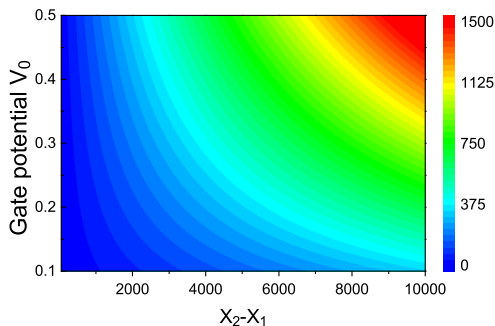


FIG. 4. (color online). Amplification factor of RKKY interaction vs. gate voltage and spin-spin distance.

demonstrates that except for the translational symmetry and Fermi surface matching, the hidden quantum mirage effect is robust against other details of the interface.

As a consequent of the distance-independent response, the carrier-mediated RKKY interaction $J\hat{\mathbf{S}}_1 \cdot \hat{\mathbf{S}}_2$ between two magnetic moments $\hat{\mathbf{S}}_1$ (located at \mathbf{R}_1) and $\hat{\mathbf{S}}_2$ (located at \mathbf{R}_2) is expected to decay with inter-spin distance $R \equiv |\mathbf{R}_2 - \mathbf{R}_1|$ as $J \propto 1/R$. Indeed, the scaled RKKY interaction strength JR shows similar distance-independent behaviors in both sharp [Fig. 3(c)] and smooth [Fig. 3(d)] PNJs, even in the presence of on-site disorder [dashed lines in Fig. 3(d)]. This indicates the robust $1/R$ decay of the RKKY interaction in graphene PNJs, as opposed to the rapid $1/R^2$ decay in uniform graphene (or $1/R^3$ decay in uniform undoped graphene). This $1/R$ scaling could dramatically amplify the RKKY interaction in graphene PNJs compared with that in uniform graphene.

Maximal amplification is achieved when the hidden quantum mirage becomes visible in a sharp PNJ satisfying Fermi surface matching. The RKKY interaction attains its maximum value J_{\max} when the second magnetic moment locates at the quantum mirage of the first magnetic moment. Extensive numerical simulation for

different $\mathbf{R}_1, \mathbf{R}_2$ and junction potential V_0 shows that in the linear dispersion regime ($V_0 \leq 1$) and for long inter-spin distances $R \gg \lambda_F$, the maximal RKKY interaction $J_{\max} \approx CV_0^2/R$, where C is a constant. For comparison, in uniform graphene with the same carrier concentration (i.e., Fermi energy $|E_F| = V_0$), the magnitude of the RKKY interaction $J_0 \approx 3CV_0/R$. Therefore, the PNJ amplifies the RKKY interaction by a factor

$$\eta = \frac{J_{\max}}{J_0} \approx \frac{V_0 R}{3}$$

that could reach three orders of magnitudes (Fig. 4). For a typical junction potential $V_0 = 1$ eV [40] and two substitutional manganese spins separated by 16 nm, their RKKY $J \sim 16$ μeV (amplified by a factor $\eta \approx 13$) is measurable by spin-polarized scanning tunneling spectroscopy [36]. When the distance increases up to the ballistic length ~ 1 μm [41], the RKKY interaction $J \sim 0.3$ μeV (amplified by a factor $\eta \approx 780$) may be detected by an ultrasensitive magnetic sensor based on nitrogen-vacancy center in nanodiamonds [47, 48], which has demonstrated nanoscale spatial resolution and the capability to determine weak magnetic dipolar interaction $\sim 10^{-5}$ μeV between two nuclear spins [49, 50].

In summary, we have proposed a robust, hidden quantum mirage that could dramatically enhance the non-local responses of electrons as well as the carrier-mediated interaction. This effect also applies to electromagnetic waves and other matter waves such as cold atoms. It may be useful for engineering energy, charge, and spin transport as well as carrier-mediated long-range correlation.

This work was supported by the MOST (Grant No. 2015CB921503, and No. 2014CB848700) and NSFC (Grant No. 11434010, No. 11274036, No. 11322542, and No. 11404043). J. J. Z. thanks the new research direction support program of CQUPT. We acknowledge the computational support from the Beijing Computational Science Research Center (CSRC).

-
- [1] V. G. Veselago, Soviet Physics Uspekhi **10**, 509 (1968).
 - [2] J. B. Pendry, Phys. Rev. Lett. **85**, 3966 (2000).
 - [3] X. Zhang and Z. Liu, Nat Mater **7**, 435 (2008).
 - [4] J. B. Pendry, A. Aubry, D. R. Smith, and S. A. Maier, Science **337**, 549 (2012).
 - [5] H. C. Manoharan, C. P. Lutz, and D. M. Eigler, Nature **403**, 512 (2000).
 - [6] V. M. Shalaev, Nat Photon **1**, 41 (2007).
 - [7] G. Juzeliunas, J. Ruseckas, M. Lindberg, L. Santos, and P. Öhberg, Phys. Rev. A **77**, 011802 (2008).
 - [8] M. Leder, C. Grossert, and M. Weitz, Nat Commun **5**, 3327 (2014).
 - [9] V. V. Cheianov, V. Fal'ko, and B. L. Altshuler, Science **315**, 1252 (2007).
 - [10] C.-H. Park, Y.-W. Son, L. Yang, M. L. Cohen, and S. G. Louie, Nano Lett. **8**, 2920 (2008).
 - [11] A. G. Moghaddam and M. Zareyan, Phys. Rev. Lett. **105**, 146803 (2010).
 - [12] L. Zhao, P. Tang, B.-L. Gu, and W. Duan, Phys. Rev. Lett. **111**, 116601 (2013).
 - [13] G.-H. Lee, G.-H. Park, and H.-J. Lee, Nat. Phys. **11**, 925 (2015).
 - [14] Z. Igor, J. Fabian, and S. Das Sarma, Rev. Mod. Phys. **76**, 323 (2004).
 - [15] C. Cirac, R. T. Hill, J. J. Mock, Y. Urzhumov, A. I. Fernandez-Domnguez, S. A. Maier, J. B. Pendry, A. Chilkoti, and D. R. Smith, Science **337**, 1072 (2012).
 - [16] V. V. Cheianov and V. I. Fal'ko, Phys. Rev. Lett. **97**, 226801 (2006).
 - [17] E. H. Hwang and S. Das Sarma, Phys. Rev. Lett. **101**, 156802 (2008).
 - [18] C. Bena, Phys. Rev. Lett. **100**, 076601 (2008).

- [19] M. A. Ruderman and C. Kittel, Phys. Rev. **96**, 99 (1954).
- [20] T. Kasuya, Prog. Theor. Phys. **16**, 45 (1956).
- [21] K. Yosida, Phys. Rev. **106**, 893 (1957).
- [22] T. Dietl and H. Ohno, Rev. Mod. Phys. **86**, 187 (2014).
- [23] J. Spector, H. L. Stormer, K. W. Baldwin, L. N. Pfeiffer, and K. W. West, Appl. Phys. Lett. **56**, 1290 (1990).
- [24] P. V. Parimi, W. T. Lu, P. Vodo, and S. Sridhar, Nature **426**, 404 (2003).
- [25] N. Fang, H. Lee, C. Sun, and X. Zhang, Science **308**, 534 (2005).
- [26] Z. Liu, H. Lee, Y. Xiong, C. Sun, and X. Zhang, Science **315**, 1686 (2007).
- [27] H. J. Lezec, J. A. Dionne, and H. A. Atwater, Science **316**, 430 (2007).
- [28] C. M. Soukoulis, S. Linden, and M. Wegener, Science **315**, 47 (2007).
- [29] T. Xu, A. Agrawal, M. Abashin, K. J. Chau, and H. J. Lezec, Nature **497**, 470 (2013).
- [30] A.-P. Li, K. W. Clark, X.-G. Zhang, and A. P. Baddorf, Advanced Functional Materials **23**, 2509 (2013).
- [31] A. Bannani, C. A. Bobisch, and R. Mller, Review of Scientific Instruments **79**, 083704 (2008).
- [32] P. W. Sutter, J.-I. Flege, and E. A. Sutter, Nat Mater **7**, 406 (2008).
- [33] S.-H. Ji, J. B. Hannon, R. M. Tromp, V. Perebeinos, J. Tersoff, and F. M. Ross, Nat Mater **11**, 114 (2012).
- [34] S. Datta, *Electronic Transport in Mesoscopic Systems* (Cambridge University Press, Cambridge, England, 1995).
- [35] R. Wiesendanger, Rev. Mod. Phys. **81**, 1495 (2009).
- [36] L. Zhou, J. Wiebe, S. Lounis, E. Vedmedenko, F. Meier, S. Blugel, P. H. Dederichs, and R. Wiesendanger, Nat. Phys. **6**, 187 (2010).
- [37] J.-J. Zhu, D.-X. Yao, S.-C. Zhang, and K. Chang, Phys. Rev. Lett. **106**, 097201 (2011).
- [38] A. A. Khajetoorians, J. Wiebe, B. Chilian, S. Lounis, S. Blugel, and R. Wiesendanger, Nat. Phys. **8**, 497 (2012).
- [39] A. F. Young and P. Kim, Nat. Phys. **5**, 222 (2009).
- [40] J. R. Williams, T. Low, M. S. Lundstrom, and C. M. Marcus, Nat Nano **6**, 222 (2011).
- [41] P. Rickhaus, P. Makk, M.-H. Liu, E. Tovari, M. Weiss, R. Maurand, K. Richter, and C. Schonenberger, Nat. Commun. **6**, 7470 (2015).
- [42] J. S. Ross, P. Klement, A. M. Jones, N. J. Ghimire, J. Yan, M. G., T. Taniguchi, K. Watanabe, K. Kitamura, W. Yao, D. H. Cobden, and X. Xu, Nat Nano **9**, 268 (2014).
- [43] B. W. H. Baugher, H. O. H. Churchill, Y. Yang, and P. Jarillo-Herrero, Nat Nano **9**, 262 (2014).
- [44] A. Pospischil, M. M. Furchi, and T. Mueller, Nat Nano **9**, 257 (2014).
- [45] Z. Zeng, T. A. Morgan, D. Fan, C. Li, Y. Hirono, X. Hu, Y. Zhao, J. S. Lee, J. Wang, Z. M. Wang, S. Yu, M. E. Hawkrige, M. Benamara, and G. J. Salamo, AIP Advances **3**, 072112 (2013).
- [46] T. Bathon, S. Achilli, P. Sessi, V. A. Golyashov, K. A. Kokh, O. E. Tereshchenko, and M. Bode, arXiv:1512.06554 [cond-mat.mes-hall] (2015).
- [47] J. R. Maze, P. L. Stanwix, J. S. Hodges, S. Hong, J. M. Taylor, P. Cappellaro, L. Jiang, M. V. G. Dutt, E. Togan, A. S. Zibrov, A. Yacoby, R. L. Walsworth, and M. D. Lukin, Nature **455**, 644 (2008).
- [48] J. M. Taylor, P. Cappellaro, L. Childress, L. Jiang, D. Budker, P. R. Hemmer, A. Yacoby, R. Walsworth, and M. D. Lukin, Nat. Phys. **4**, 810 (2008).
- [49] N. Zhao, J.-L. Hu, S.-W. Ho, J. T. K. Wan, and R.-B. Liu, Nat. Nanotechnol. **6**, 242 (2011).
- [50] F. Shi, X. Kong, P. Wang, F. Kong, N. Zhao, R.-B. Liu, and J. Du, Nat. Phys. **10**, 21 (2014).